M. Griffiths,[1] *J. F. Mecke,*[2] *and J. E. Winegar*[2]

Evolution of Microstructure in Zirconium Alloys During Irradiation

REFERENCE: Griffiths, M., Mecke, J. F., and Winegar, J. E., **"Evolution of Microstructure in Zirconium Alloys During Irradiation,"** *Zirconium in the Nuclear Industry: Eleventh International Symposium, ASTM STP 1295*, E. R. Bradley and G. P. Sabol, Eds., American Society for Testing and Materials, 1996, pp. 580–602.

ABSTRACT: X-ray diffraction (XRD) and transmission electron microscopy (TEM) have been used to characterize microstructural and microchemical changes produced by neutron irradiation in zirconium and zirconium alloys. Zircaloy-2, Zircaloy-4, and Zr-2.5Nb alloys with differing metallurgical states have been analyzed after irradiation for neutron fluences up to 25×10^{25} $n.m^{-2}$ ($E > 1$ MeV) for a range of temperatures between 330 and 580 K.

Irradiation modifies the dislocation structure through nucleation and growth of dislocation loops and, for cold-worked materials in particular, climb of existing network dislocations. In general, the **a**-type dislocation structure tends to saturate at low fluences ($<1 \times 10^{25}$ $n.m^{-2}$). The **c**-component dislocation structure, however, may evolve over long periods of irradiation (for fluences $>10 \times 10^{25}$ $n.m^{-2}$ in some cases).

The phase structure is also modified by irradiation. The common alloying/impurity elements, Fe, Cr, and Ni, are relatively insoluble in the α-phase but are dispersed into the α-phase during irradiation irrespective of the state of the phase initially containing these elements, i.e., metastable β-phase or stable intermetallic precipitate. The stable intermetallic particles may undergo structural changes dependent on their composition and the temperature. For the metastable dual-phase α/β-alloys (Zr-2.5Nb alloy), the β-phase structure is modified during irradiation, but the change is complex, being a combination of thermal decomposition and radiation-induced mixing.

KEY WORDS: zirconium, niobium, Zircaloy, zirconium alloys, microstructure, microchemistry, neutron irradiation, radiation damage, dislocation density, lattice parameters

The physical and chemical properties of Zr alloys are modified by the microstructural changes that occur in the reactor environment. It is therefore necessary to assess how the microstructure evolves during service in the nuclear reactor to predict future trends in properties. It is particularly important for structural components expected to remain in the reactor core for the life of the reactor (or until refurbishment occurs). In this paper, the microstructure of structural components from power reactors will be characterized as a function of fluence. All fluences quoted will be for neutrons with $E > 1$ MeV.

The two main alloy types used for nuclear reactor structural components are either based on Zr-Sn (Zircaloy-2 and -4) or Zr-Nb (Zr-2.5Nb). Zircaloy-2 was used for pressure tubes in the Winfrith Steam Generating Heavy Water Reactor (SGHWR) and in early CANDU[3] reactors; however, the current standard material for pressure tubes in CANDU reactors is Zr-2.5Nb. Zircaloy-2 is still used in CANDU reactors as guide tubes for control rods and flux detectors and for the calandria tubes that separate the hot Zr-2.5Nb pressure tubes from the cool mod-

[1] Staff scientist and [2] technologists, Atomic Energy of Canada Limited, Chalk River Laboratories, Chalk River, Ontario, Canada, K0J 1J0.

[3] *CA*Nada *D*euterium *U*ranium.

erator in the calandria vessel. Most of the structural core components in pressurized water reactors (PWRs) and boiling water reactors (BWRs) are fabricated from Zircaloy-2 or Zircaloy-4.

The Zircaloys are predominantly Sn rich (about 1.5 wt% Sn) α-phase materials with Fe, Cr, and Ni present in intermetallic precipitates. Zr-2.5Nb alloys are normally fabricated with a dual phase α/β structure, the α-phase being supersaturated in Nb (0.5 to 1 wt% Nb); the remaining Nb (and Fe or Cr impurities) is present in a metastable β-phase (about 20 wt% Nb, 1 wt% Fe, and 0.2 wt% Cr). The Zr-2.5Nb-alloy is also sometimes used in a heat-treated state and then reduced to a primarily α-phase structure containing precipitates of β-Nb and a few ZrNbFe-type intermetallic precipitates such as $(Zr,Nb)_3Fe$, $(Zr,Nb)_2Fe$, or $Zr(Nb,Fe)_2$ [*1*].

Experimental

X-Ray diffraction (XRD) and transmission electron microscopy (TEM) have been used to characterize microstructural and microchemical changes produced by neutron irradiation of various Zr alloy components. Both unirradiated and irradiated materials were prepared and examined. For the irradiated materials, care had to be taken to minimize the volume of material used because of the residual radioactivity in the samples.

XRD specimens that were about 1 cm^2 area by 0.5 mm thick were prepared by cutting slices out of the component perpendicular to each of three principal component axes. These axes are illustrated for typical tubular components made from Zircaloy and Zr-2.5Nb in Fig. 1, together with basal plane pole figures and schematic representations showing the preferred orientation of the α-grains. The specimens were labeled according to the direction of the normal to each slice, i.e., longitudinal normal (LN), transverse normal (TN), and radial normal (RN). Each specimen was then chemically polished to remove any damaged layer introduced by the preparation. In this case at least 0.025 mm was removed, that being the depth of damage for the diamond wheel used to cut the specimen. TEM specimens were prepared by punching 3-mm-diameter disks from 0.1-mm-thick slices. Thin foils were then made by electropolishing using a Materials Science Northwest twin-jet apparatus with a solution of 10% perchloric acid in methanol at about 230 K and a current density of about 1 $A.cm^{-2}$.

The network dislocations in the hexagonal close-packed (hcp) α-phase of Zr alloys primarily have Burgers vectors of $\frac{1}{3}\langle 11\bar{2}0\rangle$(**a**-type) or $\frac{1}{3}\langle 11\bar{2}3\rangle$(**c**+**a**-type) and [0001] (**c**-type). The latter **c**-component network dislocations have large Burgers vectors and consist of double half planes. Irradiation results in the formation of dislocation loops that have a single half-plane and Burgers vectors of: $\frac{1}{3}<11\bar{2}0$ (**a**-type), especially at low fluences and temperatures; $\frac{1}{6}\langle 20\bar{2}3\rangle$(**c**/2+**p**-type) or $\frac{1}{2}$[0001] (**c**/2-type), especially at high fluences and temperatures. The latter radiation-induced **c**-component dislocations can also be produced by climb of existing **c**-component network dislocations, primarily on basal planes. Dislocation densities were determined from line-broadening analysis using those X-ray diffraction lines having the maximum intensity for each specimen orientation. Typical errors for dislocation densities, determined from repeat measurements of the same specimen, were <4%. For the hcp α-phase, measurements were made from the Type I $\{10\bar{1}0\}$ and Type II $\{11\bar{2}0\}$ prism planes (**a**-component dislocations) and from basal (0002) planes (**c**-component dislocations) [*2*]. Because intergranular residual stresses also affect line broadening [*2,3*] and therefore the accuracy in terms of an absolute value of dislocation density, integral breadths will be used to show trends in line-broadening behavior that represent changes in dislocation densities. Typical errors for integral breadths, determined from repeat measurements of the same specimen, were <1%. Values of dislocation densities, where quoted, then represent an estimate based on prior calibrations [*2*].

Crystallographic planar spacings were determined from the peak positions using the average of peak maximum and center of gravity measurements. The α-phase **a**-type lattice parameters

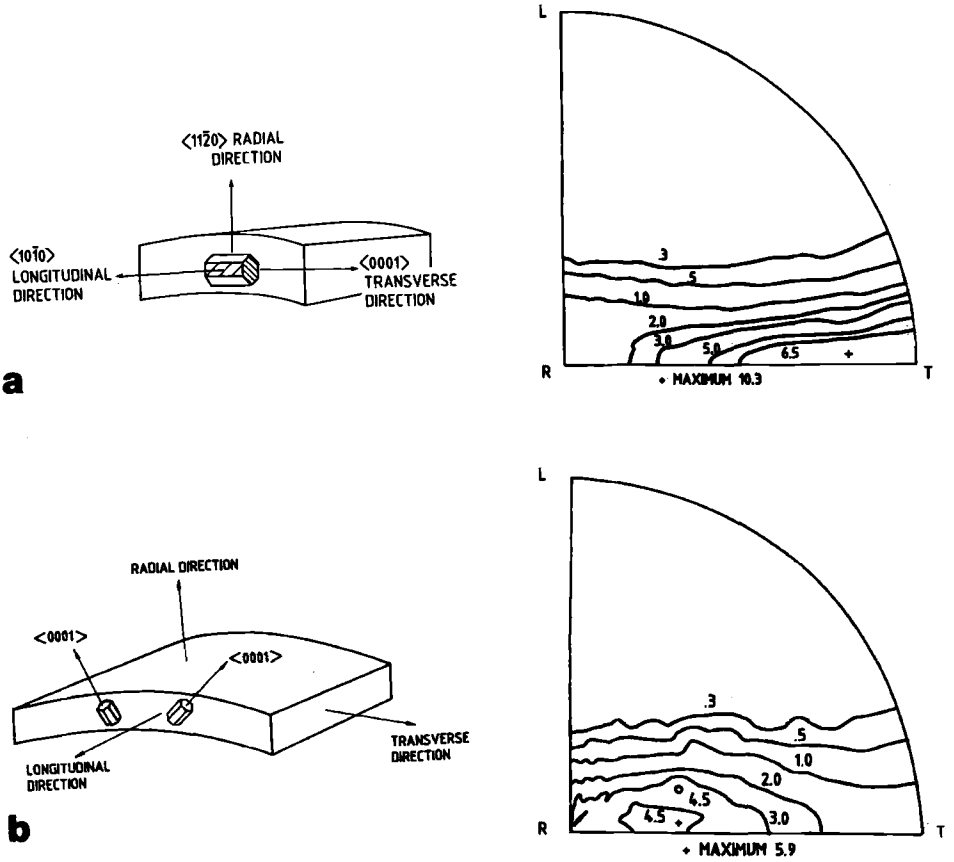

FIG. 1—*Schematic diagrams and basal pole figures illustrating the orientation of most grains in typical Zr alloy reactor core components:* (a) *Zr-2.5Nb pressure tube;* (b) *Zircaloy-4 guide tube.*

were calculated from the $\{11\bar{2}0\}$ or $\{10\bar{1}0\}$ diffraction peaks, and the c-type lattice parameters were calculated from the {0002} diffraction peaks. The β-phase lattice spacings were calculated from the (200) and (110) diffraction peaks. For Zr-2.5Nb pressure tubes, the Nb concentration in the body-centered-cubic (bcc) β-phase was then estimated from the β-phase diffraction peaks [*3*]. Typical errors for lattice parameters, determined from repeat measurements of the same specimen, were <1%. The various diffraction peaks were measured using a Rigaku or a Siemens diffractometer. CuK_α radiation (wavelength = 0.154 nm) was used in each case. The specimens were rotated in the focusing plane to increase the scanning area and sample as many grains as possible.

The state of the dislocation structure, the phase morphology, and the microchemical distribution were studied by TEM. Analysis was performed using a Philips CM 30 (300-kV) electron microscope. Microchemical analyses were obtained by energy dispersive X-ray analysis (EDXA) using a Link ISIS analyzer system and super atmospheric thin window (SATW) detector and by parallel electron energy loss spectrometry (PEELS) using a Gatan Peels analyzer. The spatial resolution for microchemical analysis was between 10 to 40 nm depending on specimen thickness. After correcting for background and self-generated X-ray signals (from

neutron-irradiated materials), relative errors for chemical composition based on repeat measurements of the same sample were generally <5%.

Results

Dislocation Structure

For all zirconium alloys, irradiation results in the formation of **a**-type loops. They are intrinsic to Zr, forming in the pure material as well as in the alloys. Their size and density are primarily dependent on the irradiation temperature. Both interstitial and vacancy loops are formed, but the relative proportions of each type are determined by the irradiation temperature and the presence of other microstructural features (grain boundaries, network dislocations, **c**-component loops, etc.) [*4*]. Recent analysis of loops in single-crystal Zr irradiated at 573 K shows that equal numbers of vacancy and interstitial loops are formed. For unalloyed polycrystalline Zr, the relative numbers of vacancy **a**-type loops decreases as the temperature is increased above 573 K [*5*]. The same observation applies to annealed Zircaloy-2 and -4 irradiated at temperatures at and above 573 K [*4*].

For annealed Zircaloy-2 components operating at about 330 to 350 K (calandria tubes and guide tubes in CANDU reactors), the radiation damage is in the form of **a**-type loops that are <5 nm in diameter. There is some evidence from post-irradiation annealed specimens to suggest that interstitial loops are more prevalent at these low temperatures (<350 K) [*4*], although there are no direct analyses to confirm this. From X-ray diffraction line broadening, calculations indicate that the **a**-type dislocation density increases from about 0.1 (as-received) to about 1 x 10^{14} m^{-2} after a fluence of about 3 $\times$ 10^{25} $n.m^{-2}$. There is no significant increase in the measured **c**-component dislocation density (typically remaining within the range of 0.01 to 0.1 $\times$ 10^{14} m^{-2}), and there is no evidence of **c**-component loop formation from TEM analysis for fluences up to about 2.5 $\times$ 10^{26} $n.m^{-2}$. For the same type of alloy operating at about 570 K (Zircaloy-4 guide tubes in PWRs and channel boxes in BWRs), the **a**-type loops are larger, about 10 to 20 nm in diameter, and are the primary form of radiation damage at low fluences. X-ray diffraction line-broadening calculations indicate that the **a**-type dislocation density in PWR guide tubes increases from about 0.1 (as-received) to about 8 $\times$ 10^{14} m^{-2} (irradiated) after a fluence of about 1 $\times$ 10^{25} $n.m^{-2}$ at about 570 K. The higher apparent **a**-type dislocation density at the higher temperature, compared with material irradiated at about 350 K, may reflect differences in the strain fields from the bounding dislocations when the loops are small, there being a lower net strain per unit length of dislocation line at the lower temperatures. In contrast to the lower temperature case, **c**-component defects in the form of basal plane dislocation loops having vacancy character are observed in annealed Zircaloy-4 irradiated at about 570 K after an incubation period of about 3 $\times$ 10^{25} $n.m^{-2}$ [*6,7*]. In this latter case, the **c**/2 dislocation density calculated from X-ray line broadening increases from an initial value of about 0.01 to 0.1 $\times$ 10^{14} m^{-2} (pre-breakaway) at a rate of about 5 $\times$ 10^{-13} n^{-1} (post-breakaway). The **c**-type dislocation density evolves over much longer periods compared with the saturating **a**-type dislocation density as illustrated by plotting prism and basal plane line broadening as a function of fluence (Fig. 2). Saturation in the prism plane broadening (**a**-type dislocation loop density) occurs after a low fluence ($\leq$1 $\times$ 10^{25} $n.m^{-2}$); however, there are insufficient high fluence data to show when the saturation in basal plane broadening (**c**-type dislocation loop density) will occur. There is an acceleration in the rate of irradiation growth corresponding with the increase in **c**-type dislocation density [*8*], and theoretical calculations show that this acceleration will continue until the **a**- and **c**-type dislocation densities are approximately equal [*9*].

For cold-worked Zircaloy-2 and -4, the **a**-type loops appear from TEM observations to be formed in similar numbers compared with the annealed materials at temperatures between about

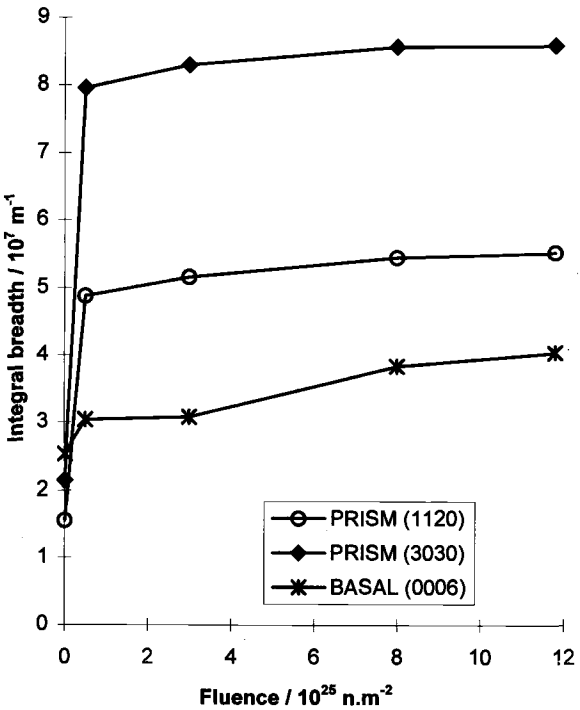

FIG. 2—*Variation in integral breadths as a function of neutron fluence for Zircaloy-4 guide tubes irradiated at 560 to 580 K using RN(11$\bar{2}$0), LN(20$\bar{2}$0), and TN(0004) specimens cut perpendicular to the radial, longitudinal, and transverse axes of the tube, respectively (see text).*

330 and 580 K. There are no data concerning XRD analysis of **a**-type dislocations and dislocation loops in 25% cold-worked Zircaloy-2 irradiated at 330 K; however, basal plane line-broadening measurements indicate that the **c**-component dislocation density increases from about 0.4×10^{14} m^{-2} to about 0.8×10^{14} m^{-2} after a fluence of 7.4×10^{25} $n.m^{-2}$, assuming that the additional dislocations are the same as the **c**-component network dislocations and have double half-planes. TEM analysis shows that there is a corresponding increase in the number of basal plane segments of **c**-component dislocations in the neutron-irradiated material (Fig. 3). Electron irradiation experiments [*10,11*] have shown that these basal plane segments can be attributed to helical climb on screw dislocations that had been generated initially by cold working. On this basis, they are likely to have single half-planes, i.e., having a **c**/2-component (**c**/2 or **c**/2+**p**), and the increment in dislocation density will be four times the value calculated as if the dislocations were **c** or **c** + **a** [*2,9*]. The screw-type **c**-component network dislocations provide nucleation sites for the climb on the basal plane, producing helices. This is especially clear when one examines grains with and without pre-existing **c**-type screw dislocations. Grains without **c**-component network dislocations do not contain basal plane **c**-component loops. This is consistent with the results for annealed material irradiated at the same low temperature, i.e., there are no new **c**-component dislocation loops nucleated at low temperatures (<350 K).

For 25 to 30% cold-worked Zircaloy-2 pressure tube material irradiated at about 550 to 580 K, the **a**-type dislocation density increases from about 2×10^{14} m^{-2} (as-received) to about 8×10^{14} m^{-2} after a fluence of about 1×10^{25} $n.m^{-2}$. The steady-state density of **a**-type defects

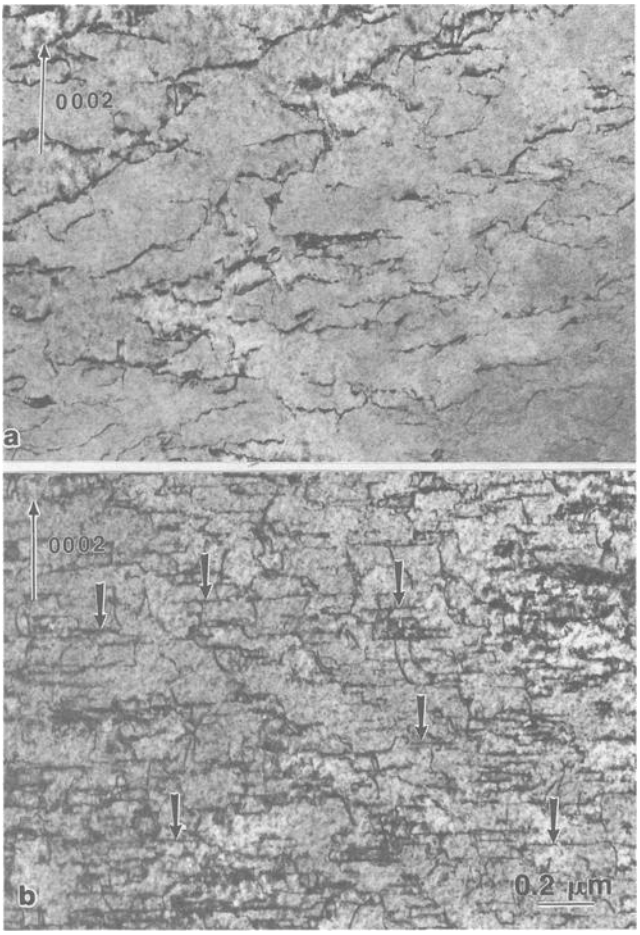

FIG. 3—*Comparison of* **c***-type dislocation structures in Zircaloy-2* (a) *before and* (b) *after irradiation to a fluence of* 7.2×10^{25} $n.m^{-2}$ *at about 330 K. Edge segments (arrowed) are produced during irradiation.*

in the irradiated cold-worked material is similar to that observed for annealed material at the same temperature. The development of basal plane **c**-component dislocation segments (by helical climb) that is observed at about 330 to 350 K in cold-worked Zircaloy-2 is also observed for cold-worked Zircaloy-2 irradiated at about 550 to 580 K [*8,9*]. As with the low temperature case, this is explained by helical climb on pre-existing **c**-component screw dislocations. Contrary to the indications of previous work [*4*]; **c**-type dislocation loop formation, i.e., separate from the screw network dislocations, can also occur at the higher temperature (550 to 580 K) and is especially apparent close to intermetallic precipitates in grains where the original **c**-component network dislocation density is low. This preferential formation of **c**-component loops close to $Zr(Cr,Fe)_2$ intermetallic precipitates is similar to that observed for the annealed material [*8*]. Therefore, there are two mechanisms for increasing **c**-component dislocation density: (1) by helical climb on existing network dislocations; (2) by dislocation loop formation.

The former occurs at the onset of irradiation, whereas the latter may be delayed if there is an incubation period for loop formation. The two contributions are apparent when comparing the behavior of cold-worked and annealed material. The relative change in basal line broadening (**c**-type dislocation density) with increasing fluence for annealed and cold-worked Zircaloy-2 irradiated at about 550 to 580 K is shown in Fig. 4. The overall rate of increase in calculated **c**/2-component dislocation density for the cold-worked material in Fig. 4 is about 2.5×10^{-12} n^{-1} and is about an order of magnitude greater than the post-breakaway rate calculated for the annealed material (5×10^{-13} n^{-1}).

There are few published data concerning the effect of irradiation on dislocation structures in annealed Zr-2.5Nb because, in the majority of cases, Zr-2.5Nb is used in a cold-worked condition. The main use of cold-worked Zr-2.5Nb is in pressure tubes in CANDU reactors. They contain the hot primary coolant operating at 520 to 570 K and are separated from the cold moderator (350 K) by a gas gap and a Zircaloy-2 calandria tube. Irradiation results in the production of a high density of small (about 15 nm in diameter) **a**-type dislocation loops. There is no clear evidence for **c**-component loop formation during irradiation at about 520 to 570 K. X-ray diffraction analysis shows that there is an increase in **a**-type (prism plane) line broadening with neutron fluence, i.e., in the core of the reactor, whereas very little appears to be happening to the **c**-type (basal) line broadening (Fig. 5). There is a variation in prism plane broadening along the tubes [*12*] that can be attributed to **a**-type dislocation loop formation with a higher density of loops at the cooler inlet end (about 520 K) compared with the hotter outlet end (about 570 K). Calculations show that the corresponding dislocation densities are about 8 ×

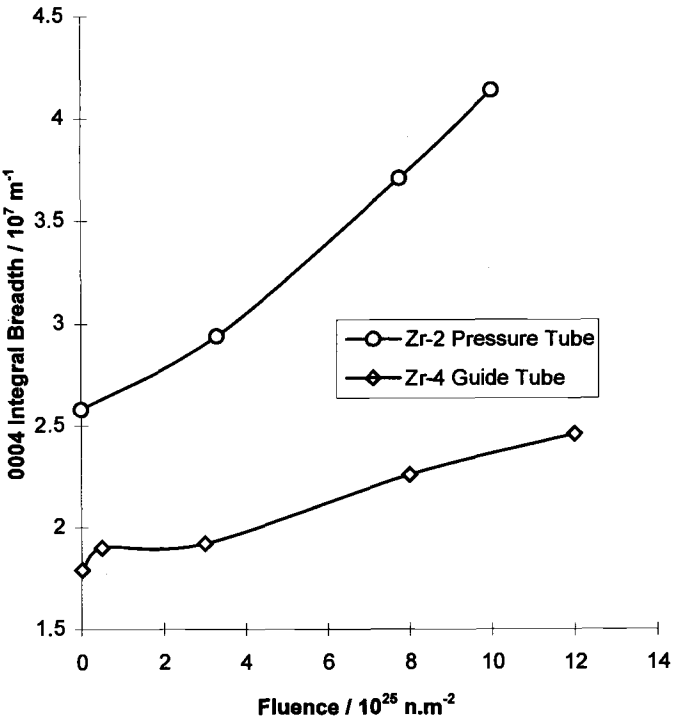

FIG. 4—*Variation in basal line broadening as a function of neutron fluence at about 570 K for annealed Zircaloy-4 guide tubes and cold-worked Zircaloy-2 pressure tubes using RN(1120).*

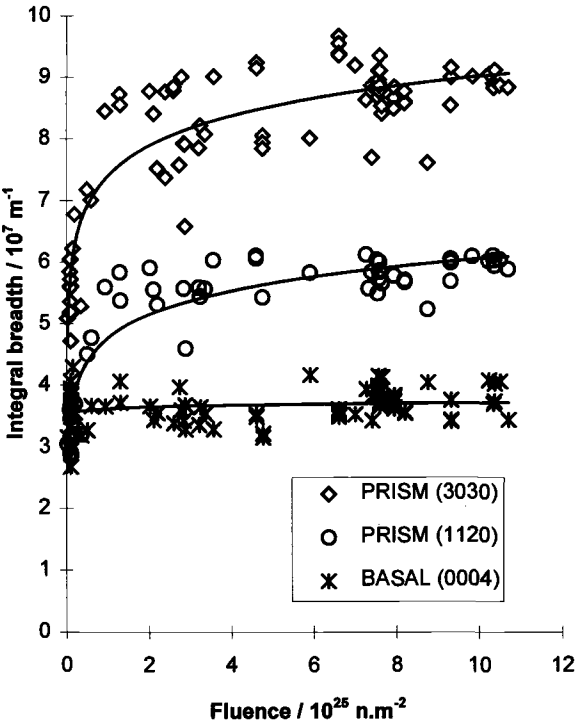

FIG. 5—*Variation in integral breadths as a function of neutron fluence in Zr-2.5Nb pressure tubes at about 520 to 570 K using RN(1120), LN(2020), and TN(0004), where RN, LN, and TN refer to specimens cut perpendicular to the radial, longitudinal, and transverse axes of the tube (see text).*

10^{14} and 6×10^{14} m^{-2}, respectively, being similar to the values obtained from cold-worked Zircaloy-2 pressure tubing. There is an apparent slight sharpening in the basal lines in the irradiated part of the tubes that can be explained by splitting of **c**-component dislocations. This type of splitting is readily observed during in situ irradiations in a high voltage electron microscope (HVEM) [*10,11*]. In general, the **a**-type dislocation density changes tend to saturate by fluences of about 1×10^{25} $n.m^{-2}$ and are somewhat similar to that observed in 25 to 30% cold-worked Zircaloy-2 [*9*] for the majority of the grains. However, the basal plane line broadening shows an increase for the Zircaloy-2 pressure tube material, indicating an increase in **c**-type dislocation density not apparent in the Zr-2.5Nb pressure tube material. This may be related to differences in susceptibility to basal plane climb or to differences in behavior of grains as a function of their orientation [*9*].

Second Phase Structure

At about 330 to 350 K, the $Zr(Cr,Fe)_2$ and $Zr_2(Ni,Fe)$ intermetallic precipitates, and also silicides, in Zircaloy-2 or -4 become amorphous. The amorphous transformation occurs at low fluences ($<1 \times 10^{25}$ $n.m^{-1}$) [*13*].

At irradiation temperatures of about 570 K, the $Zr_2(Ni,Fe)$ precipitates remain crystalline, whereas the $Zr(Cr,Fe)_2$ precipitates become amorphous [*13–17*]. In the latter case, the amorphous transformation begins at the edge of the precipitate and advances inwards with increasing

fluence. There is also a depletion of Fe coincident with the amorphous zones and a corresponding increase in concentration of Cr and Zr (Fig. 6). The concentration profile within the precipitates has two distinct zones corresponding with two distinct phases (crystalline core and amorphous periphery). There is a difference in phase transformation characteristics of $Zr(Cr,Fe)_2$ precipitates in the Zircaloys in some cases. For precipitates in Zircaloy-2 irradiated in the DIDO reactor, the particle centers can also become amorphous, in addition to the amorphous peripheral layer, even at low doses (Fig. 7). In this case, because the particles become

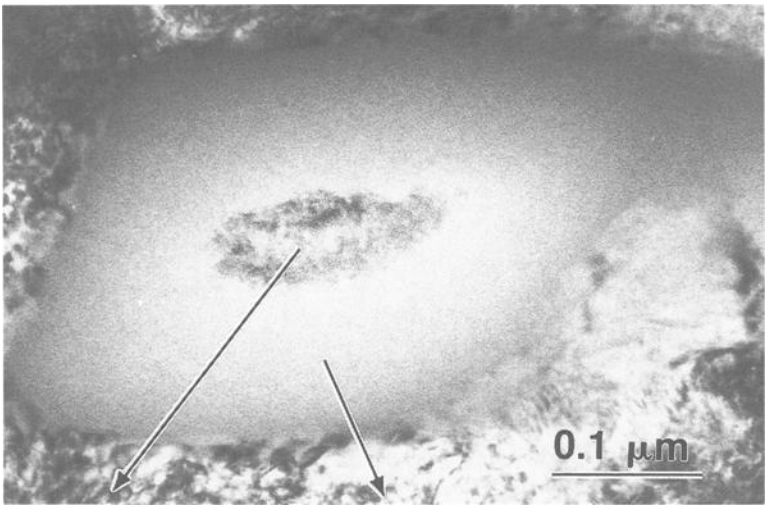

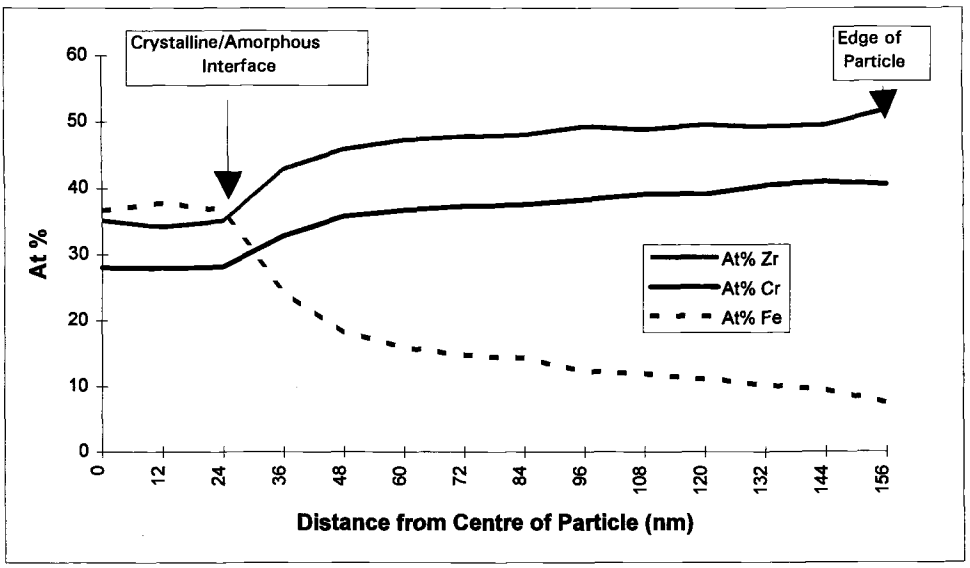

FIG. 6—*Micrograph and composition profile for a $Zr(Cr,Fe)_2$ precipitate in Zircaloy-4 irradiated at about 580 K to a fluence of 12×10^{25} n.m^{-2}. The crystalline core retains the original composition, and the amorphous peripheral layer is depleted in Fe.*

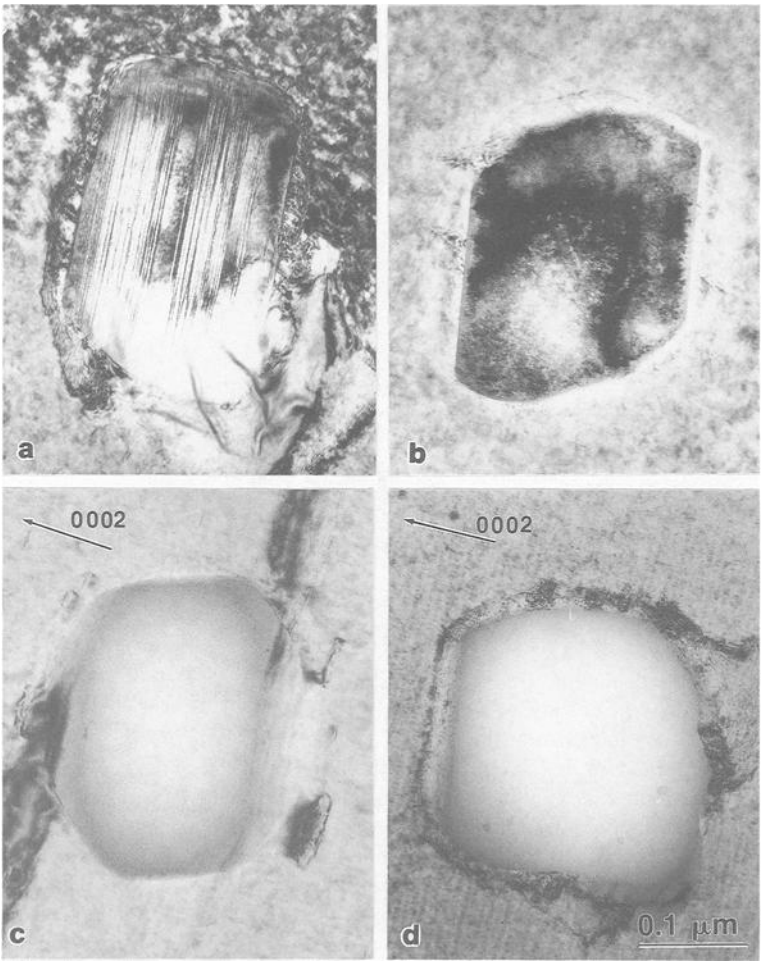

FIG. 7—*Crystalline-amorphous transformation of $Zr(Cr,Fe)_2$ intermetallic precipitates in Zircaloy-2 after irradiation at 553 K to a fluence of:* (a) 0×10^{25} *n.m*$^{-2}$; (b) 0.4×10^{25} *n.m*$^{-2}$; (c) 0.9×10^{25} *n.m*$^{-2}$; *and* (d) 2.0×10^{25} *n.m*$^{-2}$.

amorphous at a low dose, the Fe-depletion profile within the precipitate (Fig. 8) does not have the same step shape as that exhibited by the duplex crystalline/amorphous precipitates (Fig. 6). In each case, the dispersed Fe appears to be in some finely divided metastable state because post-irradiation thermal treatment below the amorphous phase recrystallization temperature results in a replenishment of Fe within the amorphous phase as the Fe diffuses back from the matrix [*18,19*]. The difference in dose to amorphous transformation may be related to the composition of the $Zr(Cr,Fe)_2$ precipitates, precipitates in Zircaloy-2 having a higher Cr,Fe ratio compared with Zircaloy-4 [*20*]. The flux may also be a factor, the precipitates shown in Fig. 7 having been irradiated in a materials test reactor (MTR) with a higher nominal flux (about 8×10^{17} n.m^2.s^{-1}) relative to a normal PWR or BWR reactor (about 6×10^{17} n.m^2.s^{-1}). This is supported by the fact that similar (Zircaloy-2) material irradiated in a lower flux CANDU reactor (about 3×10^{17} n.m^2.s^{-1}) did not become fully amorphous at the same low fluences.

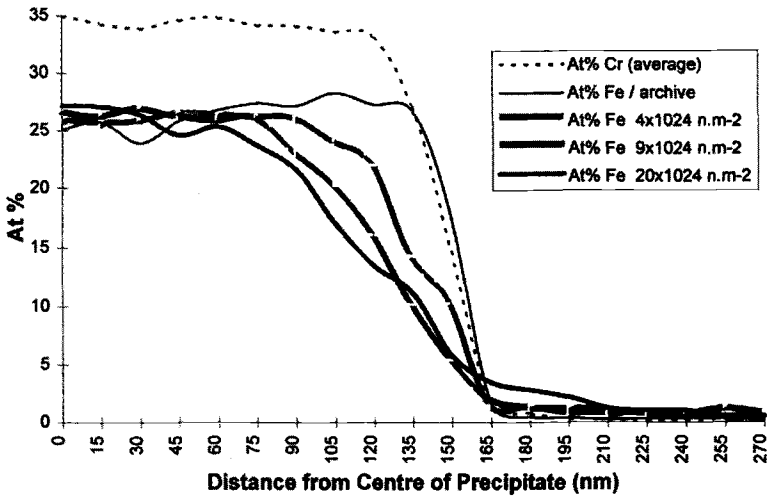

FIG. 8—*Composition profiles as a function of fluence for $Zr(Cr,Fe)_2$ precipitates in Zircaloy-2 irradiated at about 553 K. The precipitates are completely amorphous by a fluence of 0.9×10^{25} $n.m^{-2}$.*

In addition to the depletion of Fe from within the $Zr(Cr,Fe)_2$ precipitates, there is erosion at the edges of the $Zr_2(Ni,Fe)$ and $Zr(Cr,Fe)_2$ precipitates [*13–17*]. The erosion has been observed primarily on surfaces intersecting the basal plane for $Zr(Cr,Fe)_2$ precipitates [*21*]. The same directionality may exist for $Zr_2(Ni,Fe)$ precipitates also [*15–17*]. For the $Zr(Cr,Fe)_2$ precipitates, the directional erosion can be related to anisotropic dispersion of the dissolved elements (Cr and Fe), the concentration of Cr-rich precipitates forming after post-irradiation annealing being highest in regions adjacent to the $Zr(Cr,Fe)_2$ precipitates in directions parallel with the basal plane [*20*]. These same regions tend to contain a higher number of the basal plane **c**-component loops, and this may therefore be related to the local change in chemistry around the precipitates. The association between the dispersed elements and **c**-component loops is also apparent from the coincidence of the Cr and Fe, concentrated in discrete layers parallel with the basal plane, and **c**-component loops [*8*]. This localized association with the $Zr(Cr,Fe)_2$ precipitates may be linked to the fact that Cr is relatively immobile compared with Fe and Ni [*22*] and therefore maintains a higher concentration closer to the $Zr(Cr,Fe)_2$ intermetallic precipitates. There does not appear to be any association between the amorphous transformation and **c**-component loop formation, there being no evidence for **c**-component loops in the vicinity of the amorphous $Zr(Cr,Fe)_2$ precipitates shown in Fig. 7*d*.

The β-phase in Zr-2.5Nb pressure tubes is originally a single bcc phase non-equilibrium structure containing about 20 wt% Nb. It transforms to Nb- and Fe-depleted, hcp ω-phase precipitates embedded in an enriched bcc β-phase (20 to 50 wt% Nb, about 1 wt% Fe) during the final stress-relief treatment of 24, 48, or 72 h at 673 K prior to installation in the reactor (Fig. 9). This partially decomposed metastable phase continues to change during service. The concentration of Nb in the β-phase (based on the average of $\beta(200)$ and $\beta(110)$ lattice parameter measurements) can be used as a measure of the degree of decomposition and is plotted as a function of position for pressure tubes removed from service after periods ranging from 2 to 14 effective full power years in Fig. 10. A schematic flux profile is also shown in Fig. 10. The temperature increases gradually from the inlet (about 520 K) to the outlet (about 570 K), but

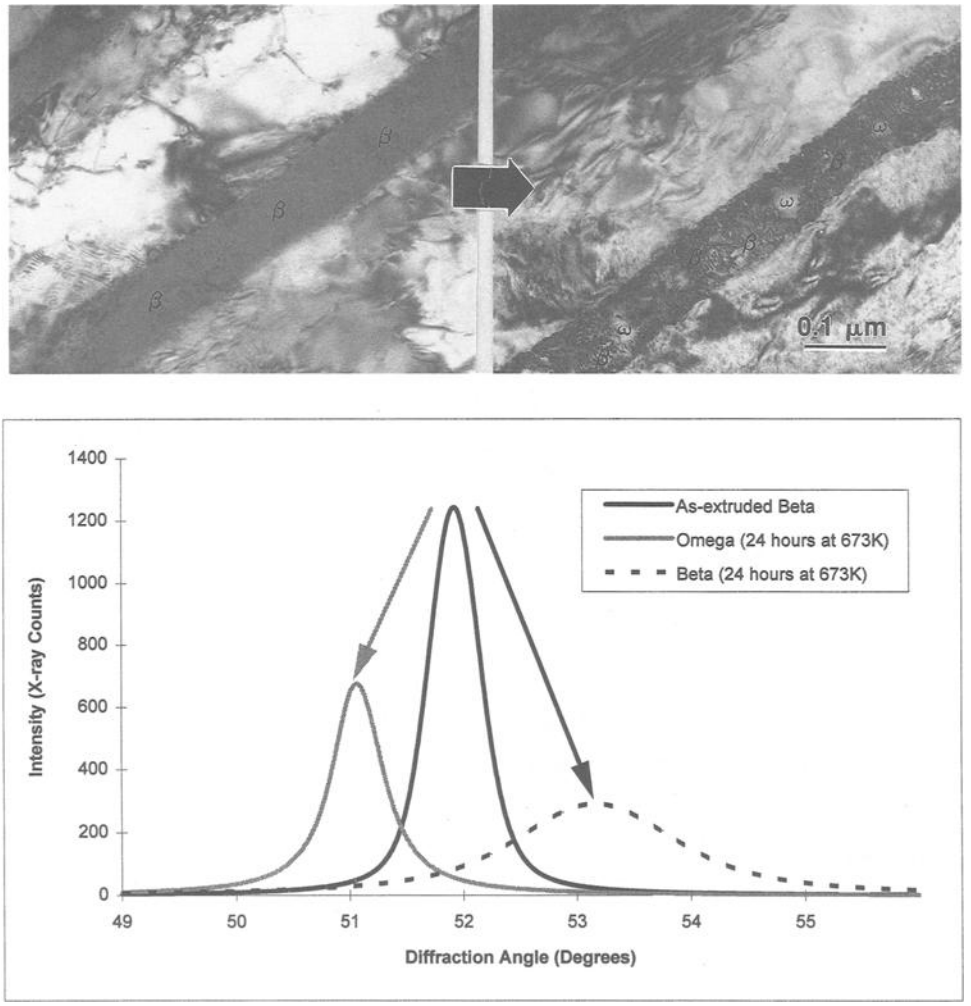

FIG. 9—*XRD diffraction lines and electron micrographs showing change in β-phase composition as a function of autoclaving heat-treatment for 24 h at 673 K. The initial single β-phase decomposes to give Nb-depleted ω-phase precipitates embedded in a Nb-enriched matrix.*

is not plotted for clarity. The scatter in the data represents variations in service time and initial tube-to-tube microstructure variations. There is an apparent Nb enrichment of the β-phase in the out-of-flux sections at each end of the tubes, and this enrichment is more pronounced at the outlet. The effect of irradiation appears to be suppression of any further thermal decomposition of the β-phase. Although there are insufficient data to make a rigorous analysis of the effects of irradiation and temperature, inspection of the data at any one position shows that there is a flux and temperature-dependent steady-state value for the composition of the β-phase achieved after about two to three years of operation. There appears to be a balance between the effects of irradiation and temperature that, of course, does not apply in the out-of-flux sections (temperature dependence only). This view is supported by measurements on specimens

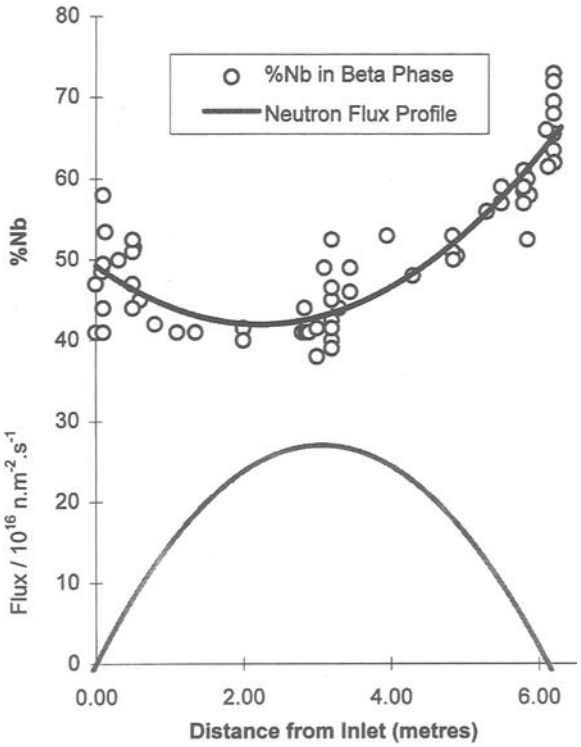

FIG. 10—*Variation in Nb composition in the β-phase as a function of position relative to the inlet for Zr-2.5Nb pressure tubes after 2 to 14 years of service. There is additional decomposition from the as-fabricated state that is apparent in the out-of-flux sections at the inlet (about 520 K) and outlet (about 570 K) but appears to be suppressed in the irradiated central section. A combined average of the RN(200) and LN(110) diffraction lines is plotted to compensate for intergranular stresses.*

that had been heat-treated for 72 h at 673 K prior to irradiation at 523 K. In this case, there was a reversal of the effects of thermal decomposition due to the low temperature irradiation (Fig. 11). The structure of the transformed β-phase is too complex to analyze using TEM; however, analysis of the X-ray peaks shows that there is an apparent decrease in volume fraction of ω-phase concurrent with the decrease in concentration of Nb in the remaining β-phase (Fig. 12). This observation is consistent with a ballistic process involving sputtering of the ω-phase precipitates. The sputtering effect appears to be more pronounced at lower temperatures, there being more evidence for increased thermal decomposition at the outlet ends (about 570 K) compared with the inlet ends (about 520 K) of the pressure tubes (Fig. 10). The net effect of temperature and neutron flux is consistent with the mechanism for precipitate redistribution proposed by Nelson et al. [*23*] involving a balance between the rate of radiation-induced dissolution and the rate of growth due to radiation-enhanced and thermal diffusion.

The Fe in the β-phase is dispersed during irradiation at temperatures between 520 and 570 K to the point where it is indistinguishable from the Fe content in the α-phase after a fluence of about 3×10^{25} n.m^{-2}. Fe is retained in the β-phase in the out-of-flux sections; Fe-rich phases are even observed after long periods of service, particularly in the region of the outlet rolled joints (Fig. 13*a*) [*12*]. Post-irradiation annealing for 1 h at 773 K reverses the flow of Fe in the

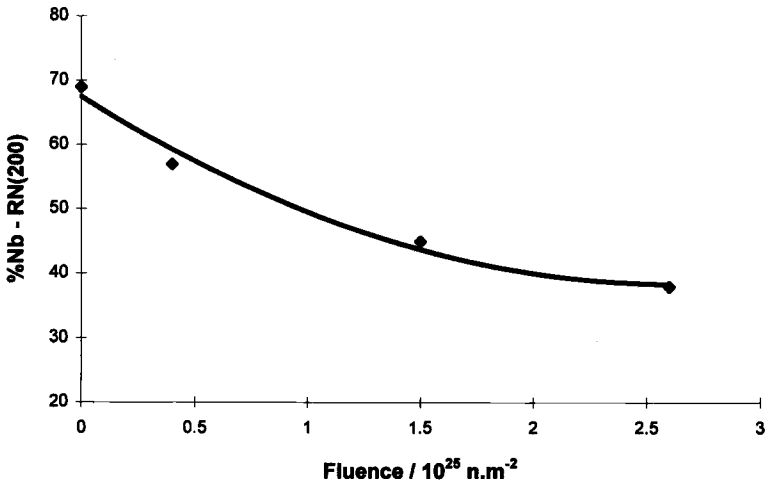

FIG. 11—*Variation in Nb composition in the β-phase (from the RN(200) diffraction lines) as a function of neutron fluence for Zr-2.5Nb pressure tube material irradiated at about 520 K in an MTR.*

irradiated material, the Fe returning to the β-phase (Fig 13*b*). The Fe dispersion is not determined by the metastable state of the β-phase because the same effect is observed for stable (Zr,Nb,Fe,Cr)-containing precipitates in heat-treated Zr-2.5Nb pressure tube material during irradiation at about 573 K. In this case, the precipitates behave somewhat similarly to the $Zr(Cr,Fe)_2$ precipitates in the Zircaloys in that there is a preferential depletion of Fe during irradiation (Fig. 14). Preliminary analysis has shown that the precipitates initially appear to be $(Zr,Nb)_3(Fe,Cr)$, consistent with the observations of Shishov et al. [*1*]. Analysis of 0.2-μm-diameter precipitates irradiated to a fluence of 1.5×10^{25} n.m^{-2} at 570 K shows that the Fe concentration is uniformly depleted, decreasing from about 20 at% in the unirradiated material to about 4 at% after irradiation, which is somewhat faster (as a function of fluence) than the depletion observed for amorphous $Zr(Cr,Fe)_2$ precipitates in Zircaloy-2 irradiated at a similar temperature (Fig. 8). There are corresponding structural changes, the precipitates decomposing to give a polycrystalline structure (Fig. 15).

Summary of Results

The significant new results presented in this paper are summarized below:

1. The dislocation loop structure in Zircaloy-2 and -4 irradiated with neutrons at low temperatures (330 to 350 K) is **a**-type only for fluences up to 2.5×10^{26} n.m^{-2}. Although **c**-component loops are not apparent in annealed material up to high fluences, irradiation of cold-worked Zircaloys containing **c**-component network dislocations (about 0.4×10^{14} m^{-2} initially) results in an additional **c**-component, i.e., **c**/2, dislocation density increase of about 1.6×10^{14} m^{-2} after a fluence of about 7.5×10^{25} n.m^{-2} due to helical climb on the existing network.
2. The **a**-type dislocation loop structure generated in annealed Zircaloy-4 at about 560 to 580 K increases rapidly in the early stages of irradiation ($<0.5 \times 10^{25}$ n.m^{-2}) from about 0.1×10^{14} m^{-2} to achieve approximate steady-state values of about 8×10^{14} m^{-2}. The **c**-type dislocation loop structure develops over a longer period. After an initial incubation

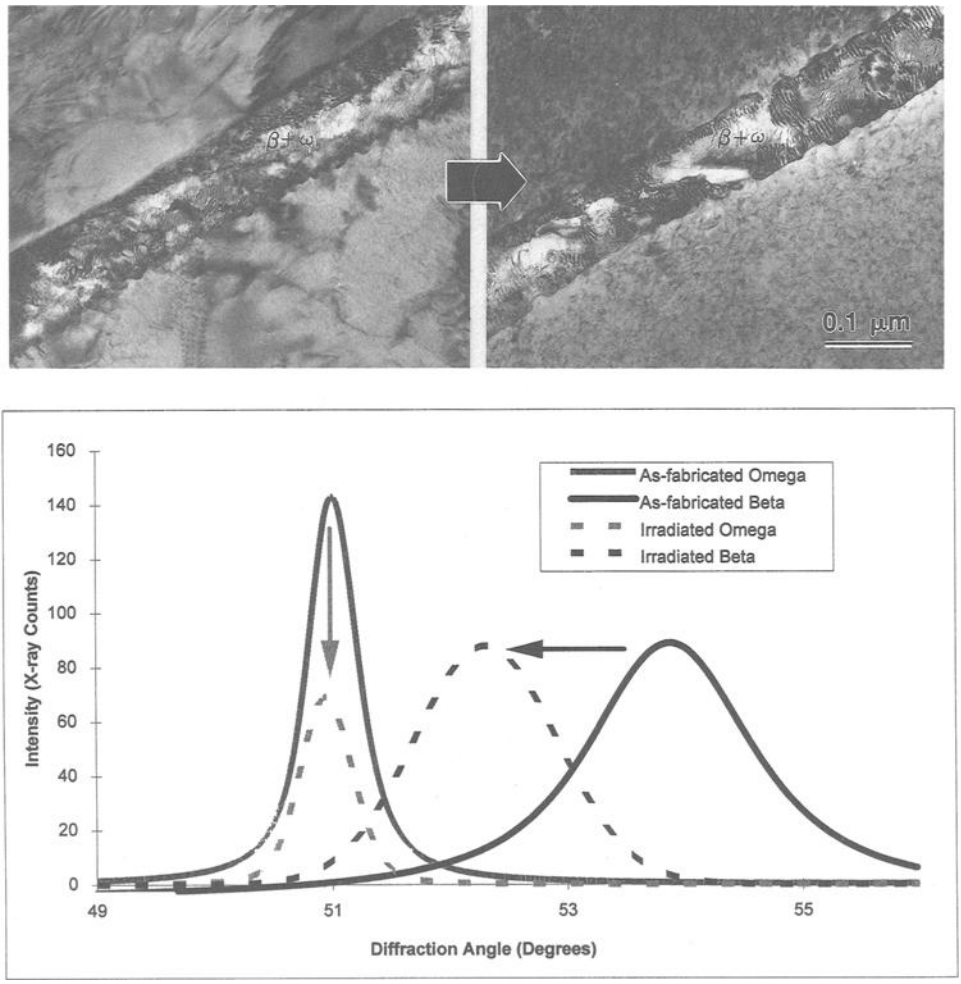

FIG. 12—*XRD diffraction lines and electron micrographs showing change in β-phase composition (for material that had been heat-treated for 72 h at 673 K) as a function of irradiation at about 520 K to a fluence of 2.6 × 10^{25} n.m^{-2}. The ω-phase volume fraction decreases coincidentally with a decrease in Nb concentration in the remainder of the filament.*

period lasting about 3 × 10^{25} n.m^{-2}, the **c**-component loop density increases from an initial value of about 0.01 to 0.1 × 10^{14} m^{-2} (pre-breakaway) at a rate of about 5 × 10^{-13} n^{-1} (post-breakaway).

3. The **a**-type dislocation loop structure generated in 25% cold-worked Zircaloy-2 pressure tubes at about 560 K is similar to that generated in 25% cold-worked Zr-2.5Nb pressure tubes at the same temperature and achieves a steady state value of about 8 × 10^{14} m^{-2}, similar to that of annealed Zircaloys irradiated at similar temperatures. The **c**-component dislocation structure measured in grains corresponding to the peak basal pole texture (radial orientation for Zircaloy-2 pressure tubes and transverse orientation for Zr-2.5Nb pressure tubes) is different in each case. Whereas the **c**-component, i.e., **c**/2, dislocation

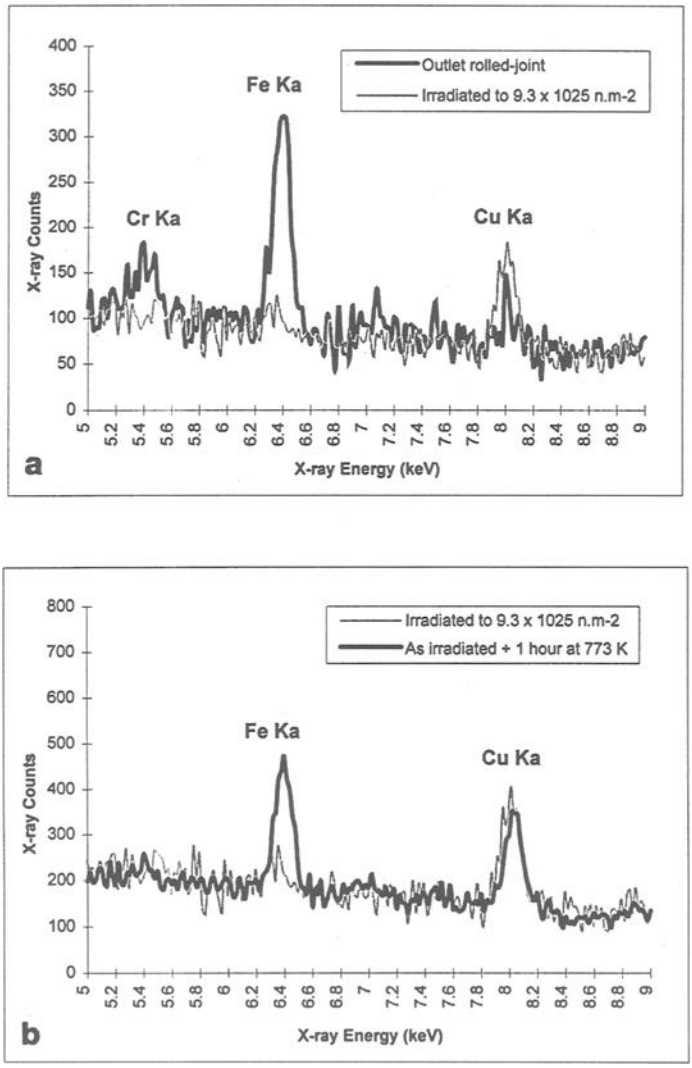

FIG. 13—*EDX spectra showing:* (a) *Fe concentration in the β-phase in an out-of-flux (at a temperature of about 570 K) and in-flux section (irradiated to a fluence of 9.3 × 10^{25} at 544 K) of a cold-worked Zr-2.5Nb pressure tube;* (b) *Fe concentration in the β-phase for an in-flux section of the same tube before and after post-irradiation annealing for 1 h at 773 K.*

density increases at a rate of about 2.5 × 10^{-12} n^{-1} in the Zircaloy-2 case, the Zr-2.5Nb material exhibits little, if any, change.

4. The transformed β-phase in as-fabricated Zr-2.5Nb pressure tubes consists of hcp ω-precipitates embedded in an Nb-enriched bcc matrix. Neutron irradiation at about 520 K with a flux of about 2 × 10^{18} $n.m^{-2}.s^{-1}$ results in mixing of the two components.
5. Irradiation of Zr alloys results in the redistribution of small-sized impurity or alloying elements such as Fe, Ni, and Cr from second phases into the primary α-phase. This

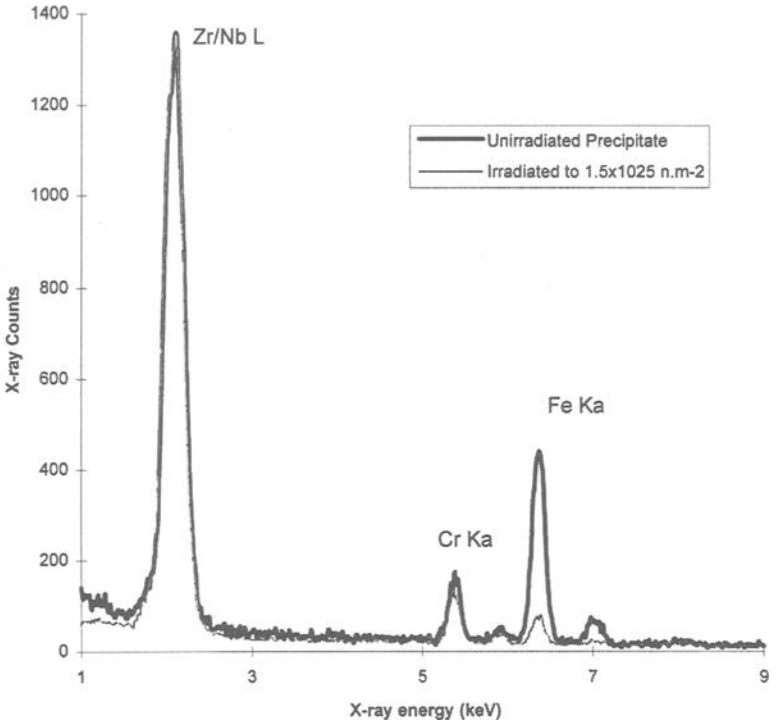

FIG. 14—*EDX spectra from the center of (Zr, Nb, Fe, Cr)-containing intermetallic precipitates in heat-treated Zr-2.5Nb before and after irradiation to a fluence of 1.6 × 10^{25} at 570 K.*

redistribution occurs irrespective of the form of the phase containing the impurity elements, and the redistribution can be reversed by post-irradiation annealing. For Fe, the rate of depletion from (Zr,Nb,Fe,Cr)-containing intermetallics in Zr-2.5Nb alloys is higher than that observed for Zr,Cr,Fe-type intermetallics in Zircaloy-2.

Discussion

The microstructural changes that occur in nuclear reactor components can have a profound effect on the service life of the individual component or even the reactor itself. Many of the important physical properties that characterize the performance of any one component, for example deformation (creep and growth), corrosion, fracture toughness, and hydrogen uptake, can change as a result of microstructure evolution during service.

For Zr-2.5Nb pressure tube materials, there is a change in fracture properties with irradiation corresponding with the evolution of the **a**-type dislocation structure [*24*]. The formation of a high density of **a**-type dislocation loops is important for modifying fracture and tensile properties. In general, the increased loop density results in a harder material with a corresponding lower fracture toughness compared with the unirradiated state. The dislocation density, strength, and fracture toughness each approach a saturation value for fluences less than 1×10^{25} n.m^{-2} [*24*]. The fact that annealed Zircaloy-4 also exhibits the same rapid increase in **a**-type dislocation at low fluences to achieve a saturated steady-state value, as shown by the line-broadening data (Fig. 2), suggests that this material will also exhibit the same trend in tensile and fracture

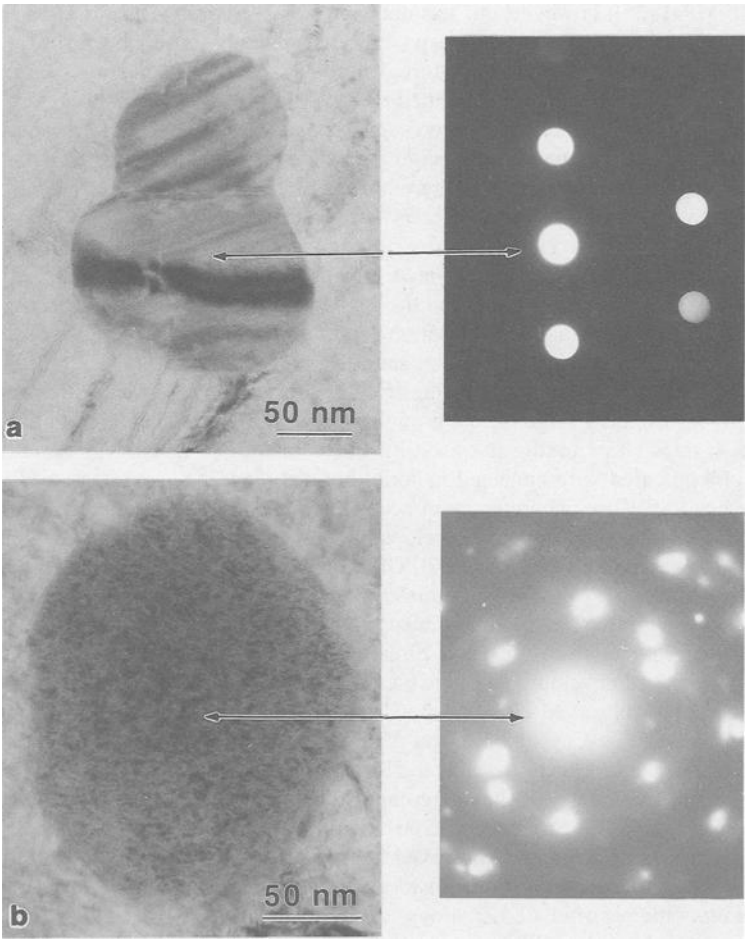

FIG. 15—*Structure of (Zr, Nb, Fe, Cr)-containing intermetallic precipitates in:* (a) *unirradiated heat-treated Zr-2.5Nb;* (b) *heat-treated Zr-2.5Nb irradiated to a fluence of* 1.6×10^{25} *n.m*$^{-2}$ *at 570 K.*

properties, achieving saturation at the same time as the **a**-type dislocation density. The role of radiation-induced **c**-component defects on tensile and fracture properties of Zr-2.5Nb and the Zircaloys has not been clearly established, there being insufficient data as a function of fluence to show whether there is a change in mechanical properties corresponding with the evolution of the **c**-component loop structure.

The dislocation structure is also important for irradiation creep and growth. Although creep rates are enhanced in a neutron flux [*25*], post-irradiation testing of irradiated material shows that thermal creep rates are reduced in pre-irradiated material, especially for material that was originally in an annealed state, and can be related to the effect of hardening. This hardening effect saturates at fluences of about 0.4×10^{25} n.m^{-2} [*25*] and is consistent with the saturation in the **a**-type dislocation loop density. There is some evidence to indicate that in-reactor creep rates for cold-worked Zr-2.5Nb at about 570 K may increase with increasing fluence at high

stresses (246 MPa) [*25*]; however, this has not been observed at lower stresses in later experiments [*26*], indicating that non-linear creep (strain localization) may be occurring at the higher stresses. There is also some low-temperature data to suggest that in-reactor creep rates at 330 K are increased for Zircaloy-4 pre-irradiated to high fluences at about 580 K, i.e., in a post-breakaway state [*27*]. The latter observation suggests that the evolving **c**-component loop structure in irradiated Zircaloys may contribute to a creep enhancement; however, there are insufficient data to be conclusive. Although there are few data concerning creep variation with an evolving dislocation microstructure, there is unequivocal evidence to show that irradiation growth is very susceptible to changes in the **c**-component dislocation structure [*8*].

There are few data concerning accelerated growth in Zr-2.5Nb alloys except at high temperatures, >640 K [*28*], and in this case the higher growth rates can be directly related to appearance of basal plane faulted dislocation loops in the material. For annealed Zircaloys, there is often an initial transient strain that saturates at low fluences that may be related to a saturation in the **a**-type dislocation loop density [*4*] or relaxation of residual stresses [*29*]. This is followed by a secondary stage of low growth rates and can then develop into higher (accelerated) growth rates at increasing fluences [*8*]. For cold-worked Zircaloys, the initial growth rates are high compared with annealed material but also appear to increase steadily with increasing fluence [*8,9*]. The phenomenon of accelerated growth is associated with an increased **c**-component dislocation density that develops either as a result of loop nucleation or due to climb of existing network dislocations [*8,9*]. The **c**-component loop formation often varies from one material to another [*28*]. In any one material, there are also grain-to-grain variations that may be related to variations in local chemistry, stress, or grain orientations [*8,9,28*]. For accelerated irradiation growth in annealed Zircaloys, the existence of an incubation period is linked with the delayed development of the **c**-component loop structure. The **c**-component loop formation is initially observed close to the $Zr(Cr,Fe)_2$ intermetallic precipitates and can be related to the increase in Cr and Fe in the matrix surrounding intermetallic precipitates [*8*]. Another factor that could affect growth is the Sn concentration within the α-phase [*30*]. At the normal operating temperature of Zircaloy components (about 560 to 580 K), however, there is no evidence for changes in Sn concentration within the α-phase that could affect irradiation growth, although Sn precipitation is observed at higher temperatures (>600 K) [*4,17,20*].

Apart from the potential effect on the dislocation structure and therefore the mechanical and deformation properties of irradiated Zr alloys, the microchemical changes induced by irradiation can also affect corrosion. For Zircaloys, the main effect of irradiation at about 570 K appears to be an increase in corrosion rate; this has been related to an increase in the solute (Fe,Cr, and Ni) concentration in the matrix during irradiation [*18*]. The dissolution and dispersion of alloying elements or impurities such as Fe, Cr, and Ni is always a potential factor in modifying alloy properties at ever increasing fluences. It has already been established that for Zircaloys irradiated at about 570 K there is a preferential radiation-induced dissolution of Fe from within $Zr(Cr,Fe)_2$ intermetallic precipitates [*13–21*] and also from within $Zr_2(Ni,Fe)$ precipitates in some cases [*17,31*]. The Fe depletion is coincident with an amorphous phase transformation in the $Zr(Cr,Fe)_2$ precipitates, and the flow is reversed during post-irradiation annealing—some Fe returns to the recrystallized precipitate at high temperatures (873 K) [*17*] or to the amorphous phase at lower temperatures (<773 K) [*19,31*]. In addition to the internal depletion of Fe, there is erosion and dispersion of Cr and Fe from $Zr(Cr,Fe)_2$ precipitates [*13–21*] and Ni and Fe from $Zr_2(Ni,Fe)$ precipitates [*15–17,20*]. These elements diffuse into the α-phase and appear to be uniformly dispersed in some finely divided form.

The effect of irradiation on corrosion in Zr-2.5Nb pressure tubes is opposite to the Zircaloy case, there being a marked decrease in corrosion rate for material that has been irradiated at 520 to 570 K compared with unirradiated material [*32*]. The improvement has been related to the decrease in Nb content in the α-phase due to Nb precipitation during irradiation [*32*].

Precipitates are observed in the α-phase of cold-worked Zr-2.5Nb pressure tubes after fluences of about 1×10^{25} n.m^{-2} [*12,33,34*]. They are generally very small (5 to 10 nm) and of insufficient volume to give coherent X-ray diffraction. EDX analysis has shown that they are Nb-rich [*33*] as one might expect for precipitates forming from a solid solution supersaturated with Nb. There are no equivalent observations of Nb precipitation in the α-phase in out-of-flux sections of pressure tubes [*12*], indicating that the precipitates are the result of irradiation.

The β-phase in Zr-2.5Nb pressure tubes has a complex structure consisting of hcp, Nb- and Fe-depleted, ω-phase precipitates in a bcc Nb- and Fe-enriched matrix. The analysis of XRD data indicates that the concentration of Nb in the bcc phase decreases and the volume fraction of ω-phase decreases during irradiation at about 520 K. The net effect on the ω-phase can be described as a balance between the rate of radiation-induced dissolution and the rate of growth due to radiation-enhanced and thermal diffusion. A similar mechanism has been postulated to explain the decomposition of large ω-phase precipitates in a Zr-12Nb alloy during electron irradiation [*35*]. In addition to the internal structural changes, Fe depletion and dispersion from the metastable β-phase has been observed in irradiated Zr-2.5Nb pressure tubes at temperatures between 520 to 570 K; however, unlike the Zircaloys, the effects of dispersed Fe on physical properties has not been established. The Fe dissolution is not necessarily dependent on the stability of the β-phase because the same phenomenon is observed for stable (Zr,Nb,Fe,Cr)-containing intermetallic $(Zr,Nb)_3(Fe,Cr)$ precipitates at 573 K (Fig. 14). The Fe depletion occurs more rapidly in the latter case compared with amorphous phases in the Zircaloys irradiated at a similar temperature (Fig. 8).

The dissolution and dispersion of Fe can occur for many different Zr-alloy phases containing Fe. A number of hypotheses have been proposed to explain the phenomenon [*13–17,36*], and all depend to a large extent on diffusion of Fe into the matrix, i.e., the precipitate-matrix interface is not a barrier to diffusion. The depletion of Fe during irradiation and replenishment of Fe during post-irradiation annealing for the $Zr(Cr,Fe)_2$ intermetallic precipitates in the Zircaloys [*19*] and the β-phase in Zr-2.5Nb alloys (Fig. 13) indicates that the Fe can migrate across the interface by diffusion and that it is in a metastable state (supersaturated solid solution or in small solute clusters) in the α-phase. The recent data of Fig. 6 show that, for the $Zr(Cr,Fe)_2$ precipitates in the Zircaloys, the decrease in Fe content is coincident with an increase in Zr and Cr in approximately equal proportions. This indicates that the Fe diffuses into the matrix without being replaced by another element, e.g., by a vacancy exchange mechanism.

Conclusions

X-ray diffraction (XRD) and transmission electron microscopy (TEM) have been used to characterize microstructural and microchemical changes produced by neutron irradiation in Zircaloy-2 and -4 and Zr-2.5Nb nuclear reactor components.

1. Irradiation modifies the dislocation structure initially by nucleation and growth of **a**-type dislocation loops and, for cold-worked materials, climb of existing network dislocations. In general, the **a**-type dislocation structure tends to saturate at low fluences ($<1 \times 10^{25}$ n.m^{-2}). The **c**-component dislocation structure, however, can evolve over long periods of irradiation (for fluences $> 10 \times 10^{25}$ n.m^{-2} in many cases).

2. In Zircaloy-2 and -4, all precipitates become completely amorphous at low fluences ($<1 \times 10^{24}$ n.m^{-2}) during low-temperature neutron irradiation (about 330 K) with no associated chemical composition change. At higher temperatures (about 573 K), a duplex amorphous-crystalline structure is produced in the $Zr(Cr,Fe)_2$ precipitates, all other precipitate types remaining unchanged. The $Zr(Cr,Fe)_2$ precipitates often retain a crystalline core surrounded by a peripheral amorphous layer that advances inwards with increasing fluence. The amorphous

outer layer is coincident with a depletion of Fe that is dispersed into the surrounding hcp α-phase matrix. In some cases, depending on composition or flux, the precipitate centers can also become amorphous even at low doses. Subsequent post-irradiation heat-treatment below the amorphous phase recrystallization temperature results in the back-diffusion of Fe into the amorphous phase.

3. For Zr-2.5Nb materials, irradiation results in the formation of Nb-rich precipitates within the α-phase with a corresponding decrease of Nb in solid solution. The metastable transformed β-phase structure is modified during irradiation, but the change is complex, being a combination of thermal decomposition and radiation-induced mixing. There is dispersion of Fe from the β-phase during irradiation at temperatures between 520 and 570 K and, after a fluence of about 3×10^{25} n.m^{-2}, the β-phase Fe content cannot be distinguished from that in the α-phase matrix. Subsequent post-irradiation heat treatment, for times and temperatures that do not induce significant recrystallization of the α- or β-phase, results in the back-diffusion of Fe into the β-phase.

Acknowledgments

The authors would like to thank R. A. Holt, B. A. Cheadle, C. Lemaignan, D. Gilbon, and Y. de Carlan for many useful discussions. The authors would also like to thank R. R. Hosbons and P. H. Davies for the supply of some specimens, G. P. Smith of ABB-Combustion Engineering and O. Ozer of EPRI for permission to use unpublished data (Project No. RP-2905-02), and the CANDU Owners Group for funding under Work Package 32-3325.

References

[1] Shishov, V. N., Nikulina, A. V., Markelov, V. A., Peregud, M. M., Kozlov, A. V., Averin, S. A., Kolbenkov, S. A., and Novoselov, A. E., "Influence of Neutron Irradiation on Dislocation Structure and Phase Composition in Zr-Base Alloys," this publication.

[2] Griffiths, M., Winegar, J. E., Mecke, J. F., and Holt, R. A., "Determination of Dislocation Densities in HCP Metals using XRD and TEM," *Advances in X-ray Analysis*, C. S. Barrett et al., Eds., Plenum Press, New York, 1991, p. 593.

[3] Griffiths, M., Winegar, J. E., Mecke, J. F., Holden, T. M., and Holt, R. A., "A Comparison of X-ray and Neutron Diffraction for the Determination of Residual Stress and Chemical Composition in Zr-Alloy Tubes," *Advances in X-ray Analysis*, C. S. Barrett et al., Eds., Plenum Press, New York, 1991, p. 475.

[4] Griffiths, M., "A Review of Microstructure Evolution in Zr-Alloys during Irradiation," *Journal of Nuclear Materials*, Vol. 159, 1988, p. 190.

[5] Jostsons, A., Kelly, P. M., Blake, R. G., and Farrell, K., "Neutron-Induced Defect Structures in Zirconium," *Effects of Irradiation on Structural Materials (Ninth Conference), ASTM STP 683*, 1979, p. 46.

[6] Holt, R. A. and Gilbert, R. W., "<c> Component Dislocations in Annealed Zircaloy Irradiated at about 570 K," *Journal of Nuclear Materials*, Vol. 137, 1986, p. 185.

[7] Griffiths, M. and Gilbert, R. W., "The Formation of c-Component Defects in Zirconium Alloys during Neutron Irradiation," *Journal of Nuclear Materials*, Vol. 150, 1987, p. 169.

[8] Griffiths, M., Holt, R. A., and Rogerson, A., "Microstructural Aspects of Accelerated Deformation of Zircaloy Nuclear Reactor Components during Service," *Journal of Nuclear Materials*, Vol. 225, 1995, p. 245.

[9] Holt, R. A., Causey, A. R., Christodoulou, N., Griffiths, M., Ho, E. T. C., and Woo, C. H., "Non-Linear Deformation of Cold-Worked Zircaloy-2 During Irradiation," this publication.

[10] Griffiths, M., Styles, R. C., Woo, C. H, Philipp, F., and Frank, W., "Study of Point Defect Mobilities in Zirconium during Electron Irradiation in a HVEM," *Journal of Nuclear Materials*, Vol. 208, 1994, p. 324.

[11] Griffiths, M., Gilbon, D., Regnard, C., and Lemaignan, C., "HVEM Study of the Effects of Alloying Elements and Impurities on Radiation damage in Zr-Alloys," *Journal of Nuclear Materials*, Vol. 205, 1993, p. 273.

[12] Griffiths, M., Chow, C. K., Coleman, C. E., Holt, R. A., Sagat, S., and Urbanic, V. F., "Evolution of Microstructure in Zr-Alloy Core Components during Service," *Effects of Irradiation on Materials (Sixteenth Volume), ASTM STP 1175*, 1993, p. 1077.
[13] Gilbert, R. W., Griffiths, M., and Carpenter, G. J. C., "Amorphous Intermetallics in Neutron Irradiated Zircaloys After High Fluences," *Journal of Nuclear Materials*, Vol. 135, 1985, p. 265.
[14] Yang, W. J. S., Tucker, R. P., Cheng, B., and Adamson, R. B., "Precipitates in Zircaloy: Identification and the Effects of Irradiation and Thermal Treatment," *Journal of Nuclear Materials*, Vol. 138, 1986, p. 185.
[15] Garzarolli, F., Dewes, P., Maussner, G., and Basso, H. H., "Effects of High Neutron Fluences on Microstructure and Growth of Zircaloy-4," *Zirconium in the Nuclear Industry (Eighth International Symposium), ASTM STP 1023*, 1989, p. 641.
[16] Etoh, Y. and Shimada, S., "Neutron Irradiation Effects on Intermetallic Precipitates in Zircaloy as a Function of Fluence," *Journal of Nuclear Materials*, Vol. 200, 1993, p. 59.
[17] Gilbon, D. and Simonot, C., "Effect of Irradiation on Microstructure of Zircaloy-4," *Zirconium in the Nuclear Industry (Tenth Volume), ASTM STP 1245*, 1994, p. 521.
[18] Cheng, B., Kruger, R. M., and Adamson, R. B., "Corrosion Behaviour of Irradiated Zircaloy," *Zirconium in the Nuclear Industry (Tenth Volume), ASTM STP 1245*, 1994, p. 400.
[19] Griffiths, M., de Carlan, Y., Lefebvre, F., and Lemaignan, C., "A TEM Study of the Stability of Intermetallic Precipitates in Zircaloy Nuclear Reactor Components," to be published in *Micron*.
[20] Griffiths, M., Gilbert, R. W., and Carpenter, G. J. C., "Phase Stability, Decomposition and Redistribution of Intermetallic Precipitates in Zircaloy-2 and -4 During Neutron Irradiation," *Journal of Nuclear Materials*, Vol. 150, 1987, p. 53.
[21] Yang, W. J. S., "Precipitate Stability in Neutron Irradiated Zircaloy-4," *Journal of Nuclear Materials*, Vol. 158, 1988, p. 71.
[22] Hood, G. M., "Point Defect Diffusion in α-Zr," *Journal of Nuclear Materials*, Vol. 159, 1988, p. 149.
[23] Nelson, R. S., Hudson, J. A., and Mazey, D. J., "The Stability of Precipitates in an Irradiation Environment," *Journal of Nuclear Materials*, Vol. 44, 1972, p. 318.
[24] Davies, P. H., Hosbons, R. R., Griffiths, M., and Chow, C. K., "Correlation Between Irradiated and Unirradiated Fracture Toughness of Zr-2.5Nb Pressure Tubes," *Zirconium in the Nuclear Industry (Tenth Volume), ASTM STP 1245*, 1994, p. 135.
[25] Fidleris, V., "The Irradiation Creep and Growth Phenomenon," *Journal of Nuclear Materials*, Vol. 159, 1988, p. 22.
[26] Causey, A. R., Elder, J. E., Holt, R. A., and Fleck, R. G., "On the Anisotropy of In-Reactor Creep of Zr-2.5Nb Tubes," *Zirconium in the Nuclear Industry (Tenth Volume), ASTM STP 1245*, 1994, p. 202.
[27] Causey, A. R., Fidleris, V., and Holt, R. A., "Acceleration of Creep and Growth of Annealed Zircaloy-4 by Pre-Irradiation to High Fluences," *Journal of Nuclear Materials*, Vol. 139, 1986, p. 277.
[28] Griffiths, M., Gilbert, R. W., and Fidleris, V., "Accelerated Irradiation Growth of Zirconium Alloys," *Zirconium in the Nuclear Industry (Eighth International Symposium), ASTM STP 1023*, 1989, p. 658.
[29] Causey, A. R., Woo, C. H., and Holt, R. A., "The Effect of Intergranular Stresses on the Texture Dependence of Irradiation Growth of Zr-Alloys," *Journal of Nuclear Materials*, Vol. 159, 1988, p. 225.
[30] Rogerson, A., "Irradiation Growth in Zirconium and Its Alloys," *Journal of Nuclear Materials*, Vol. 159, 1988, p. 43.
[31] Kruger, R. M. and Adamson, R. B., "Precipitate Behaviour in Zirconium-Based Alloys in BWR's," *Journal of Nuclear Materials*, Vol. 205, 1993, p. 242.
[32] Urbanic, V. F. and Griffiths., M., "Corrosion Response of Pre-Irradiated Zr-2.5Nb Pressure Tube Material," *Proceedings*, Seventeenth International Symposium on the Effects of Irradiation on Materials, to be published.
[33] Griffiths, M. and Mullejans, H., "A TEM Study of α-Phase Stability in Zr-2.5Nb Pressure Tubes Following Neutron Irradiation," to be published in *Micron*.
[34] Coleman, C. E., Gilbert, R. W., Carpenter, G. J. C., and Weatherly, G. C., "Precipitation in Zr-2.5 Nb during Neutron Irradiation," *Stability during Irradiation*, J. R. Holland, L. K. Mansur, and D. I. Potter, Eds., AIME, 1980, p. 587.
[35] Faulkner, D. and Nuttall, K., "The Effect of Irradiation on the Stability of Precipitates in Zr-2.5Nb Alloys," *Journal of Nuclear Materials*, Vol. 67, 1977, p. 131.
[36] Motta, A. T. and Lemaignan, C., "A Ballistic Mixing Model for the Amorphization of Precipitates in Zircaloy under Neutron Irradiation," *Journal of Nuclear Materials*, Vol. 195, 1992, p. 277.

DISCUSSION

A. T. Motta[1] *(written discussion)*—In what state is the Fe in the matrix after leaving the precipitates in Zr (Cr, Fe)$_2$? If you believe that the Fe is in solid solution in the matrix, is it your belief that the solubility of Fe under irradiation in the matrix is enhanced relative to the solubility outside of irradiation?

M. Griffiths et al. (authors' closure)—All that can be said is that the Fe is in a finely dispersed form. The fact that some of the dispersed Fe returns to the parent phase during post-irradiation annealing suggests that it is in a metastable state within the α-phase. One could argue that this state is a supersaturated solid solution, although some secondary precipitation would also be expected.

S. Yagnik[2] *(written discussion)*—Since Fe reappears back in the particles upon modest annealing (500°C , ~ 1 h), it appears reasonable that Fe is in a metastable state not too far from the particle itself. Yet we have seen evidence of entirely new Fe-bearing particles forming, presumably quite a distance from the original particles, in another paper in this session. This appears to be an apparent contradiction. Please comment.

M. Griffiths et al. (authors' closure)—Not necessarily. The dispersed Fe (and Cr or Ni) will be available to form secondary precipitates, and such precipitates are readily observed at higher temperatures of irradiation (>673 K). It is likely that small secondary precipitates do exist close to the parent intermetallic particle. We do not know, however, whether the Fe that returns to the parent phase comes from re-dissolved (metastable) secondary precipitates or from a supersaturated solid solution.

B. Lehtinen[3] *(written discussion)*—Are there any "extra peaks" in the EDS spectrum due to the radiated specimen? If so, do you subtract them from the spectrum or are you using an energy filtering method?

M. Griffiths et al. (authors' closure)—Yes, self-generated X-ray peaks in neutron-irradiated Zr alloys are a problem and have to be subtracted prior to analysis of the spectrum by a hole-count method. The main extra peaks are Mn K, Zr K, and Nb K generated by election capture.

Y. Etoh[4] *(written discussion)*—Is there any correlation between Cr distribution and c-component dislocation loops near amorphous Zr-Fe-Cr particles? Is the c-dislocation a fast diffusion path for Cr?

M. Griffiths et al. (authors' closure)—Previous work has shown a correlation between impurities, such as Fe and Cr, and c-component dislocation loops. I believe that the Cr is important for enhancing c-component loop stability near intermetallic particles because it is less mobile than Fe (or Ni) and a higher local concentration is achieved. I do not know of any data to indicate that c-dislocations enhance the diffusion of Cr specifically, although one might anticipate enhanced diffusion (of all elements) along any dislocation.

[1] Pennsylvania State University, University Park, PA.
[2] Electric Power Research Institute, Palo Alto, CA.
[3] Institute of Metals Research, Stockholm, Sweden.
[4] Nippon Nuclear Fuel Development Co., Ltd., Ibataki-ken, Japan.